



1 *Conference Proceedings Paper*

## 2 **Deformation monitoring using Sentinel-1 SAR data**

3 **Núria Devanthery<sup>1,\*</sup>, Michele Crosetto<sup>1</sup>, Oriol Monserrat<sup>1</sup>, María Cuevas-González<sup>1</sup> and Bruno**  
4 **Crippa<sup>2</sup>**

5 <sup>1</sup> Centre Tecnològic de Telecomunicacions de Catalunya (CTTC/CERCA); ndevanthery@cttc.cat,  
6 mcrosetto@cttc.cat, omonserrat@cttc.cat, mcuevas@cttc.cat.

7 <sup>2</sup> University of Milan; bruno.crippa@unimi.it

8 \* Correspondence: ndevanthery@cttc.cat; Tel.: +34 936 452 900

9 Published: date

10 **Abstract:** Satellite earth observation enables the monitoring of different types of natural hazards,  
11 contributing to the mitigation of their fatal consequences. In this paper, satellite Synthetic Aperture  
12 Radar (SAR) images are used to derive terrain deformation measurements. The images acquired  
13 with the ESA satellites Sentinel-1 are used. In order to fully exploit these images, two different  
14 approaches to Persistent Scatterer Interferometry (PSI) are used, depending on the characteristics of  
15 the study area and the available images. The main processing steps of the two methods, i.e. the  
16 simplified and the full PSI approach, are described and applied over an area of 7500 km<sup>2</sup> located in  
17 Catalonia (Spain). The deformation velocity map and deformation time series are analysed in the  
18 last section of the paper.

19 **Keywords:** Deformation monitoring, Remote Sensing, Synthetic Aperture Radar, Sentinel-1,  
20 Differential SAR Interferometry, wide area processing

---

### 22 **1. Introduction**

23 Satellite observation is a key tool for the observation of the Earth, enabling, in particular, the  
24 mitigation of natural hazards' consequences. It provides several advantages over other monitoring  
25 techniques: acquisition of data in inaccessible areas; extensive coverage, which allows the complete  
26 analysis of global phenomena; and provision long-term historical data for large areas, enabling the  
27 temporal analysis of the phenomena. Additionally, it outperforms the generally more expensive and  
28 slow in situ data acquisition.

29 In this work, we use Synthetic Aperture Radar (SAR) images and Differential SAR  
30 Interferometry (DinSAR) technique to derive terrain deformation measurements. Previous works  
31 performed with the technique have been successfully carried out in the fields of geophysics,  
32 volcanology [1,2], seismology [3], landslide monitoring [4] and subsidence measurements [5]. In  
33 particular, an advanced approach to DinSAR, the Persistent Scatterer Interferometry (PSI) technique  
34 [6,7], is used. This technique uses large sets of SAR images acquired over the same area to measure  
35 the velocity of deformation of the terrain and the deformation time series (see [8] for a review of the  
36 technique).

37 A set of 36 SAR images acquired with the ESA satellites Sentinel-1 (S-1) are used in this study.  
38 S-1 acquires at C-band and brings important advantages with respect to other sensors: wide area  
39 coverage, with the Interferometric Wide Swath mode it acquires images covering 250 by 180 km;  
40 frequent revisit time of 6 days; and free of charge availability.

41 This paper is structured as follows: in Section 2 the approach to PSI used in the study is  
42 described, in Section 3 the deformation measurements are derived over the area of Catalonia  
43 (northern Spain), and in Section 4 the conclusions of the study are presented.

## 44 2. Methodology

45 The technique used in this study is an implementation of the PSI approach. In order to process  
46 the Sentinel-1 interferometric data, we use two complementary approaches, depending on the  
47 characteristics of the study area, the availability of the images, and the type of phenomenon to  
48 monitor. The two approaches are a simplified PSI method and a full PSI approach. These two  
49 approaches are described below.

### 50 2.1 Simplified PSI approach

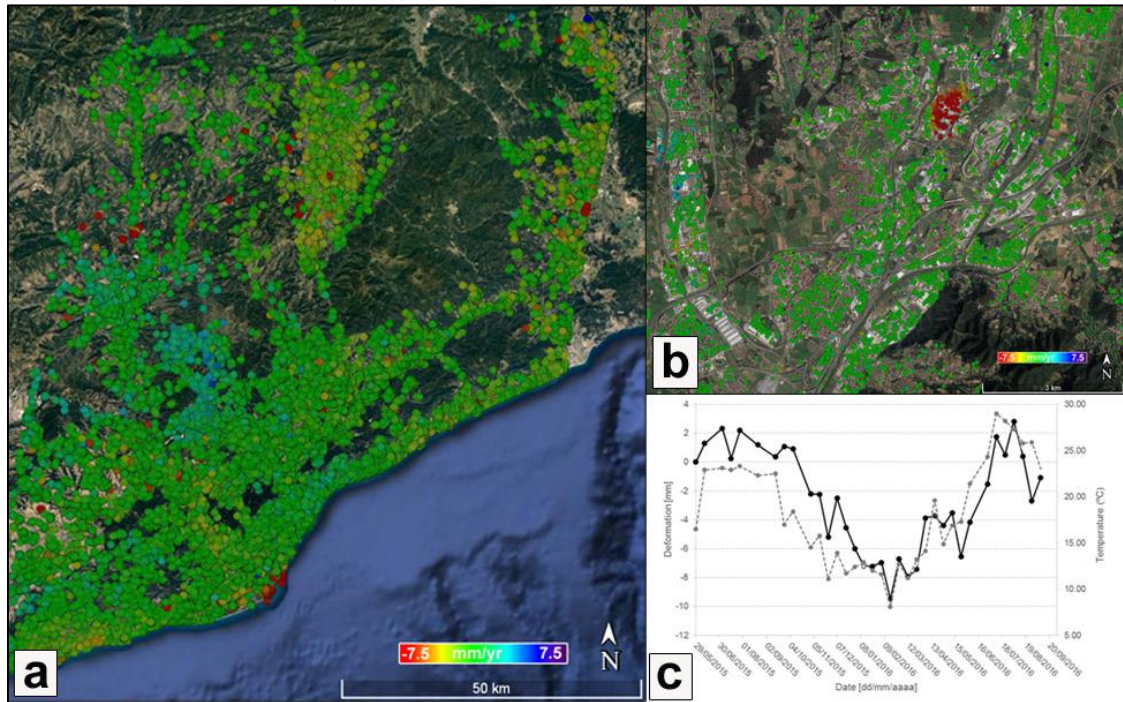
51 The simplified approach uses consecutive interferograms in order to fully exploit the increased  
52 coherence of 6-day temporal baseline interferograms. This approach is mainly used when working  
53 in non-urban areas, where the coherence decreases very fast in time. The procedure starts with a stack  
54 of  $N$  complex SAR images and  $N-1$  consecutive multi-look interferograms. The main steps are: (i) 2D  
55 phase unwrapping of the  $N-1$  multi-look interferograms, using the Minimum Cost Flow method  
56 [9,10]; (ii) Direct integration of the unwrapped interferometric phases, to obtain temporally ordered  
57 phases in correspondence to the image acquisition dates; (iii) Estimation and removal of the  
58 atmospheric phase component by means of a set of spatio-temporal filters [7,11]; (iv) Generation of  
59 the deformation time series and accumulated deformation map, using the atmosphere-free  
60 interferograms and transforming the phases into displacements; (v) Geocoding of the results.

### 61 2.2 Full PSI approach

62 The full PSI approach gives the best results when working in high coherence areas. This  
63 approach requires a large set of  $N$  SAR images and a redundant network of  $M$  interferograms, where  
64  $M \gg N$ . Their main steps are: (i) Perform the so-called 2+1D phase unwrapping. First, a spatial 2D  
65 phase unwrapping using the Minimum Cost Flow method [9,10] is performed over the multi-looked  
66 interferograms. This is followed by a 1D phase unwrapping performed pixel wise over the  $M$   
67 interferograms, which uses an iterative least squares procedure [12,13,14] that fully exploits the  
68 integer nature of the unwrapping errors. This last step is able to detect and correct the errors  
69 generated during the 2D phase unwrapping stage, and provides tools to control the quality of the  
70 derived time series [15]; (ii) Estimation of the atmospheric phase component (APS) and removal from  
71 the interferograms at full resolution. This is performed by means of a set of spatio-temporal filters;  
72 (iii) Deformation velocity and residual topographic error (RTE) estimation using the method of the  
73 periodogram; (iv) removal of the RTE phase component from the wrapped APS-free interferograms;  
74 (v) Generation of the final deformation time series by means of the final iteration of the 2+1D phase  
75 unwrapping. This involves a 2D phase unwrapping, followed by a 1D phase unwrapping; (vi)  
76 Geocoding of the results.

## 77 3. Results

78 The approaches detailed in the previous section have been used to monitor the full region of  
79 Catalonia (Spain). The velocity of deformation and time series of deformation have been derived  
80 using 36 Sentinel-1A images acquired in the Interferometric Wide Swath Mode covering the period  
81 from March 2015 to September 2016. The temporal baseline is usually 12 days, while in some cases it  
82 is 24 and 36 days. Figure 1a show the velocity of deformation map derived over an area of about 7500  
83 km<sup>2</sup> using the full PSI approach and a redundant network of interferograms. The urban areas are  
84 covered with measurements, while in most cases, the vegetated and non-urban areas lack points due  
85 to the low coherence and hence the noise of these areas.



86

87

88

89

**Figure 1.** (a) Deformation velocity map derived using 36 Sentinel-1 images during the period March 2015 to September 2016, (b) Zoom of the velocity map over a subsidence in the metropolitan area of Barcelona, (c) Deformation time series associated to thermal dilation.

90

91

92

93

94

Figure 1a shows that most of the studied area is stable (green points). However, some interesting deformations were detected from this map. Figure 1b shows a subset in the metropolitan area of Barcelona. Two differentiated areas of deformation can be appreciated, which are probably related to water extraction phenomena. In red, there is a subsidence that reaches more than 15 mm/year, while in blue there is an uplift up to 5 mm/year.

95

96

97

98

Figure 1c shows the deformation time series of a point located over an industrial building in Barcelona (black line related to the left axis). It shows a periodical movement which is related to the temperature (grey dotted line, which refers to the right axis). This time series shows the high deformation sensitivity of the measurements.

99

100

101

102

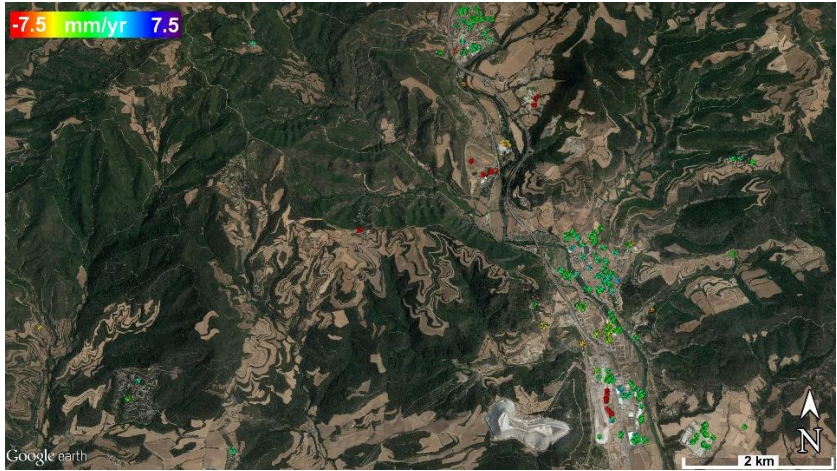
103

104

105

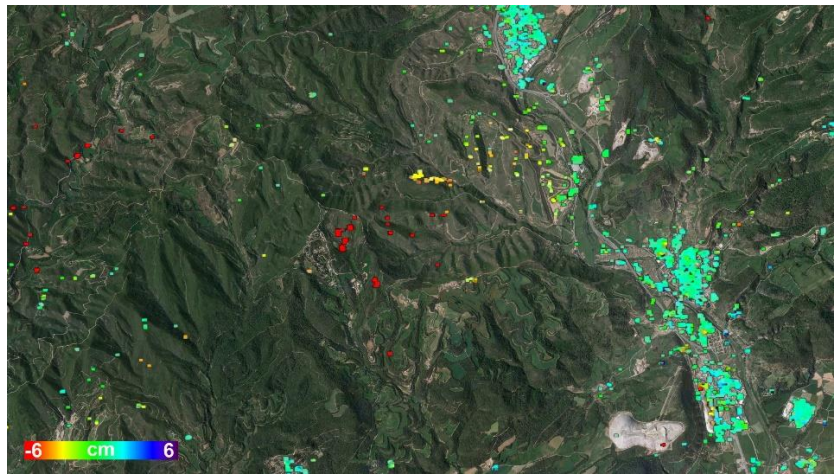
106

The best results are derived with the full PSI approach using redundancy of interferograms. However, in some areas, the density of points is not enough. In those cases, the simplified approach is used to take advantage of the high coherence of consecutive interferograms. Figures 2 and 3 show the deformation measured over an area undergoing mining activities. Figure 2 shows the velocity of deformation with a maximum of 25 mm/year of subsidence (in red). Figure 3 is the accumulated deformation map derived using the simplified approach and 24 S-1 images, spanning the period from March 2015 to January 2016. In this case, the simplified approach allows obtaining a higher measurement density over the area of interest.



107  
108  
109

**Figure 2.** Velocity map over the period March 2015 to September 2016, derived using a full PSI approach .



110  
111  
112

**Figure 3.** Accumulated deformation map using 24 Sentinel-1 images during the period March 2015 to January 2016, derived using a simplified PSI approach.

## 113 5. Conclusions

114 The deformation map over an area in Catalonia (Spain) has been derived using Sentinel-1  
115 Synthetic Aperture radar (SAR) images. Two different approaches based on Differential SAR  
116 Interferometry (DInSAR) have been used: the complete PSI procedure, which uses redundancy of  
117 interferograms and whose key step is a 2+1D phase unwrapping which allows to detect and correct  
118 phase unwrapping errors, and the simplified approach, which uses consecutive interferograms in  
119 order to take advantage of the high coherence of 12 day interferograms. Some examples of measured  
120 deformations have been shown.

121 **Acknowledgments:** This work has been partially funded by the Spanish Ministry of Economy and  
122 Competitiveness through the DEMOS project “Deformation monitoring using Sentinel-1 data” (Ref: CGL2017-  
123 83704-P).

124 **Author Contributions:** Nuria Devanthery implemented some parts of the approach and performed the study.  
125 Michele Crosetto was in charge of the scientific and technical coordination. Oriol Monserrat implemented some  
126 key parts of the approach. Maria Cuevas-Gonzalez contributed to the processing and analysis of the data. Bruno  
127 Crippa was in charge of the algorithm development.

128 **Conflicts of Interest:** The authors declare no conflict of interest.

129

130

## 131 Abbreviations

132 The following abbreviations are used in this manuscript:

133 SAR: Synthetic Aperture Radar

134 DinSAR: Differential Synthetic Aperture Radar Interferometry

135 PSI: Persistent Scatterer Interferometry

136 S-1: Sentinel-1

137 RTE: Residual topographic error

138 APS: Atmospheric Phase Screen

## 139 References

- 140 1. Antonielli, B., Monserrat, O., Bonini, M., Righini, G., Sani, F., Luzi, G., Feyzullayev, A.A., Aliyev, C.S. Pre-  
141 eruptive ground deformation of Azerbaijan mud volcanoes detected through satellite radar interferometry  
142 (DInSAR). *Tectonophysics* **2014**, 637, 163-177.
- 143 2. Massonnet, D., Briole, P., Arnaud, A. Deflation of Mount Etna monitored by spaceborne radar  
144 interferometry. *Nature* **1995**, 375, 567-570.
- 145 3. Massonnet, D., Rossi, M., Carmona, C., Adragna, F., Peltzer, G., Feigl, K., Rabaute, T. The displacement  
146 field of the Landers earthquake mapped by radar interferometry. *Nature* **1993**, 364(6433), 138-142.
- 147 4. García-Davalillo, J.C., Herrera, G., Notti, D., Strozzi, T., Álvarez-Fernández, I. DInSAR analysis of ALOS  
148 PALSAR images for the assessment of very slow landslides: the Tena Valley case study. *Landslides* **2014**,  
149 11(2), 225-246.
- 150 5. Herrera, G., Tomás, R., López-Sánchez, J.M., Delgado, J., Mallorquí, J.J., Duque, S., Mulas, J. Advanced  
151 DInSAR analysis on mining areas: La Union case study (Murcia, SE Spain). *Engineering Geology* **2007**. 90(3),  
152 148-159.
- 153 6. Ferretti, A., Prati, C. and Rocca, F. Nonlinear subsidence rate estimation using permanent scatterers in  
154 differential SAR interferometry. *IEEE TGRS* **2000**. 38(5), 2202–2212.
- 155 7. Ferretti, A., Prati, C., and Rocca, F. Permanent scatterers in SAR interferometry. *IEEE TGRS* **2001**, 39(1), 8–  
156 20.
- 157 8. Crosetto, M., Monserrat, O., Cuevas-González, M., Devanthery, N. Persistent Scatterer Interferometry: a  
158 review. *ISPRS J. of Photogrammetry and Remote Sensing* **2016**, 115, 78-89.
- 159 9. Costantini, M. A novel phase unwrapping method based on network programming. *IEEE TGRS* **1998**, 36,  
160 813–821.
- 161 10. Costantini, M., Farina, A., Zirilli, F. A fast phase unwrapping algorithm for SAR interferometry. *IEEE TGRS*  
162 **1999**. 37, 452–460.
- 163 11. Berardino, P., Fornaro, G., Lanari, R., and Sansosti, E. A new algorithm for surface deformation monitoring  
164 based on small baseline differential SAR interferograms. *IEEE TGRS* **2002**. 40(11), 2375–2383.
- 165 12. Baarda, W. A Testing Procedure for Use in Geodetic Networks. Kanaalweg 4, Rijkscommissie voor  
166 Geodesie, 1968, Delft, The Netherlands.
- 167 13. Björck, Å. Numerical Methods for Least Square Problems. Siam, 1996, Philadelphia, PA, USA.
- 168 14. Förstner, W. Reliability, gross error detection and self-calibration. ISPRS Commission III Tutorial on  
169 Statistical Concepts for Quality Control. ISPRS Int. Arch. Photogramm., 1986, 26, 1–34.
- 170 15. Devanthery, N., Crosetto, M., Monserrat, O., Cuevas-González, M., and Crippa, B. An approach to  
171 Persistent Scatterer Interferometry. *Remote Sensing* **2014**. 6(7), 6662-6679.
- 172



© 2018 by the authors; licensee MDPI, Basel, Switzerland. This article is an open access article distributed under the terms and conditions of the Creative Commons Attribution (CC-BY) license (<http://creativecommons.org/licenses/by/4.0/>).